

Nuclear effects in neutrino-nucleus interactions

Maria B. Barbaro

University of Torino and INFN, Via Giuria 1, I-10125 Torino, Italy

E-mail: Barbaro@to.infn.it

Abstract. An accurate description of the nuclear response functions for neutrino scattering in the GeV region is essential for the interpretation of present and future neutrino oscillation experiments. Due to the close similarity of electromagnetic and weak scattering processes, we will review the status of the scaling approach and of relativistic modeling for the inclusive electron scattering response functions in the quasielastic and Δ -resonance regions. In particular, recent studies have been focused on scaling violations and the degree to which these imply modifications of existing predictions for neutrino reactions. We will discuss sources and magnitude of such violations, emphasizing similarities and differences between electron and neutrino reactions.

1. Introduction

The motivation of the recent interest in neutrino-nucleus interactions is twofold. On one hand ongoing and future high precision neutrino oscillation experiments increasingly rely on our knowledge of neutrino-nucleus interactions in both Charged Current (CC) processes of the type $\nu_l + A \rightarrow l + N + (A - 1)$, where a virtual W boson is exchanged, and Neutral Current (NC) reactions $\nu_l + A \rightarrow \nu'_l + N + (A - 1)$, where a Z boson is exchanged. Typical neutrino energies involved in these experiments are of a few GeV. In this region a large contribution to the cross section comes from quasielastic and resonance processes, where the nuclear dynamics is known to play an important role. Since many electron scattering data exist at these kinematics (see Ref. [1] for a recent review), we should be able to use them to predict neutrino cross sections. As we will show, the superscaling properties of inclusive (e, e') data represent a bridge between electron and neutrino scattering reactions off nuclei.

A second motivation consists in the fact that neutrinos can reveal informations on the nuclear structure complementary to electrons and they can be used to probe the internal structure of the nucleon (in particular the axial mass and the strange form factors), providing the nuclear content of the problem is under control.

In this contribution we will first review the phenomenon of superscaling in inclusive electron-nucleus scattering [2, 3, 4, 5] and then show some predictions for ν - A cross sections based on the SuperScaling Approximation (“SuSA”) [6, 7]. We will then discuss the microscopic origin of the superscaling function, with particular focus on two models, the Relativistic Mean Field (RMF) [8] and a BCS-like correlated Fermi gas [9], which seem to correctly reproduce the shape of the (e, e') experimental data, at variance with other relativistic models. Finally we will address the issue of scaling violations, in particular the ones connected to meson-exchange currents.

2. Superscaling

The experimental quasielastic (e, e') cross sections display the so-called “first kind scaling” [5] behaviour: at high momentum transfer (q larger than about 0.5 GeV/c) the reduced quasielastic cross section

$$F = \frac{d\sigma}{d\Omega d\omega} / (Z\sigma_{ep} + N\sigma_{en}) \quad (1)$$

does not depend on two variables (q, ω) but only on one combination of them, called the scaling variable and indicated by $y(q, \omega)$ in a non-relativistic scheme and $\psi(q, \omega)$ in a relativistic context. These two scaling variables represent respectively the minimum momentum ($-y$) or kinetic energy ($m_N\psi$) that a nucleon inside the target nucleus must have in order to participate to the reaction. The conditions $y = 0$ and $\psi = 0$ correspond, in the non-relativistic and relativistic case respectively, the quasielastic peak (QEP). In Ref. [4] it was shown that if the reduced function (1) corresponding to different kinematical conditions is plotted as a function of y it fulfills with good accuracy first kind scaling in the so-called scaling region $y < 0$, whereas at $y > 0$ scaling is broken.

Second kind scaling consists instead in the observation that for different target nuclei the reduced cross section scales as the inverse of the Fermi momentum k_F , so that the so-called *superscaling function* $f = k_F \times F$ is independent of the specific nucleus. This has been illustrated in Ref. [5], where it has been shown that scaling of second kind is excellent in the scaling region and slightly violated at the right of the QEP.

If first and second kind scaling are simultaneously respected the cross sections are said to “superscale”. A closer inspection of the Rosenbluth-separated longitudinal and transverse response functions shows that the scaling violations observed at $\psi > 0$ mainly reside in the transverse channel, essentially due to the Δ resonance contribution.

Before proceeding, let us briefly remind the basic formalism for inclusive electron scattering, focussing on the longitudinal channel where superscaling is seen to work better. In plane wave impulse approximation the longitudinal quasielastic response function can be expressed as

$$R_L(q, \omega) = \frac{2\pi m_N^2}{q} \int \int_{\Sigma} dp d\mathcal{E} S(p, \mathcal{E}) \mathcal{R}_L(q, \omega; p, \mathcal{E}), \quad (2)$$

where $\Sigma(q, \omega)$ is the kinematically allowed region in the (\mathcal{E}, p) plane, \mathcal{E} being the excitation energy of the residual nucleus and p its momentum, $S(p, \mathcal{E})$ is the nuclear spectral function and \mathcal{R}_L the single nucleon response, which depends on the electric and magnetic nucleon’s form factors.

Assuming that the single nucleon response \mathcal{R}_L is smoothly varying in the (\mathcal{E}, p) -plane and can be factored out of the integral one gets

$$R_L(q, \omega) = \mathcal{R}_L(q, \omega; p = p_{\min}, \mathcal{E} = 0) \times F_L(q, \omega) \quad (3)$$

where

$$F_L(q, \omega) = \frac{2\pi m_N^2}{q} \int \int_{\Sigma(q, \omega)} dp d\mathcal{E} S(p, \mathcal{E}) \quad (4)$$

is the longitudinal scaling function. Note that the above factorization can be only approximately true in a relativistic context and it is violated to some degree due to off-shell effects and breaking of independent particle models.

The simplest model where one can perform exact relativistic calculations is the Relativistic Fermi Gas (RFG), namely an independent-particle model in which on-shell nucleons are described by Dirac spinors. In spite of its simplicity the RFG model retains some fundamental properties: it is Lorentz covariant and gauge invariant and is therefore a good starting point

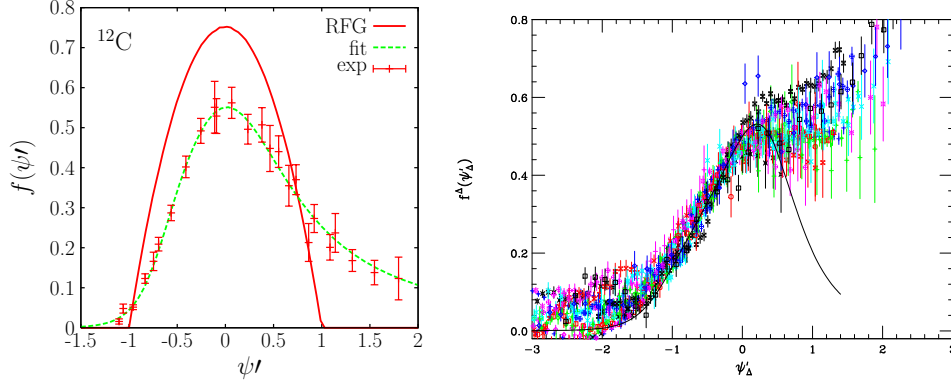


Figure 1. The experimental superscaling function in the quasielastic (left panel) [10] and Δ resonance (right panel) regions.

for more sophisticated calculations. The RFG spectral function is $S^{RFG}(p, \mathcal{E}) = \theta(k_F - p)\delta(\mathcal{E} - T_F + T_p)$ and the corresponding scaling function is

$$F_L(q, \omega) = \left(\frac{m_N}{q}\right) \left(\frac{1}{k_F}\right) \frac{3}{4} (1 - \psi^2) \theta(1 - \psi^2) \quad (5)$$

where the parabola $\frac{3}{4} (1 - \psi^2) \theta(1 - \psi^2) \equiv f(\psi)$ is the superscaling function and $\psi \equiv \psi(q, \omega)$ is the RFG scaling variable. The RFG model exactly superscales, as the data do in the so-called scaling region. However the comparison with the averaged data, illustrated in the left panel of Fig. 2, shows that the corresponding superscaling function is very different from the experimental one and in particular it fails to reproduce the long tail displayed by the data at large positive ψ . However a simple phenomenological approach can be taken for describing the QE region: a fit of the experimental superscaling function can be extracted from the data and plugged into the RFG formulas in place of the parabola (5). Note that the fit involves only four parameters for describing *all* kinematics and *all* nuclei. Moreover, it represents a strong constraint on nuclear models, since any reasonable model used to describe the quasielastic region must reproduce this shape.

The scaling analysis has been recently extended to the Δ resonance region [6]. In order to isolate the contributions in this region, the impulsive contributions arising from quasielastic eN scattering, calculated assuming superscaling is valid, has been removed from the experimental total cross section and the result has been divided by the elementary $N \rightarrow \Delta$ cross section, thus leading to a new superscaling function

$$f_\Delta(q, \psi_\Delta) \equiv k_F \frac{[d^2\sigma/d\Omega_e d\omega]_\Delta}{\sigma_M [v_L G_L^\Delta + v_T G_T^\Delta]} . \quad (6)$$

When the latter is plotted against the appropriate scaling variable $\psi_\Delta \equiv \psi(q\rho, \omega\rho)$, which accounts for the different kinematics through the inelasticity parameter $\rho = 1 + (m_\Delta^2 - m_N^2)/(4|Q^2|)$, the result shown in the right panel of Fig. 2 is obtained. Obviously this approach can work only at $\psi'_\Delta < 0$, since at $\psi'_\Delta > 0$ other resonances and the tail of DIS contribute.

The two above superscaling functions can then be used to reconstruct the (e, e') cross sections in the QE and Δ regions, giving a satisfactory description of the data, as shown in Ref. [6].

3. Predictions for neutrino scattering: the SuSA approach

We shall now illustrate how the superscaling properties of inclusive electron scattering can be exploited to predict neutrino cross sections off nuclei.

Charged current neutrino-nucleus scattering can be easily linked to inclusive (e, e') reactions by replacing the virtual photon by a virtual W -boson. The main difference is that in the neutrino case, beyond the longitudinal and transverse response functions, a third response is involved, arising from the axial component of the weak current. In the RFG model the three response functions turn out to be

$$\tilde{R}_i = \tilde{G}_i \times f(\psi) , \quad (7)$$

where the functions \tilde{G}_i depend on the weak nucleon form factors and the information about the nuclear dynamics is carried by the superscaling function $f(\psi)$. The basic assumption of the SuSA approximation is that the nuclear dynamics governing the neutrino-nucleus process is the same entering the electron scattering reactions and therefore the corresponding cross sections in the QE and Δ regions can be obtained by simply replacing in (7) the RFG superscaling function with the corresponding phenomenological fits: $f_{RFG} \Rightarrow f_{QE, \Delta}$.

In the left panel of Fig. 3 the double differential cross section in the QE and Δ regions is shown for (see Refs. [6] for more results): it clearly appears that in both regions the SuSA result lies significantly lower and extends over a wider range in k' than the RFG. In the right panel the SuSA fully integrated quasielastic cross section [11] on ^{12}C is shown as a function of the neutrino energy and compared not only with the RFG but also with other relativistic models: the relativistic mean field (RMF) model, the relativistic plane wave impulse approximation (RPWIA) and a semi-relativistic shell model without (SRWS) or with (SRWS-tot) inclusion of discrete states of ^{12}N . Note that the RMF yields results which are very similar to the SuSA prediction, whereas the other models are closer to the RFG. The comparison of these results with the recent MiniBooNE data [12], which lie above the RFG and seem to point to a very high value of the axial mass ($M_{AC}^2 = 1.35 \text{ GeV}$ in place of the usual value 1.03, which we are using in our calculations), is somehow puzzling and still needs to be carefully explored.

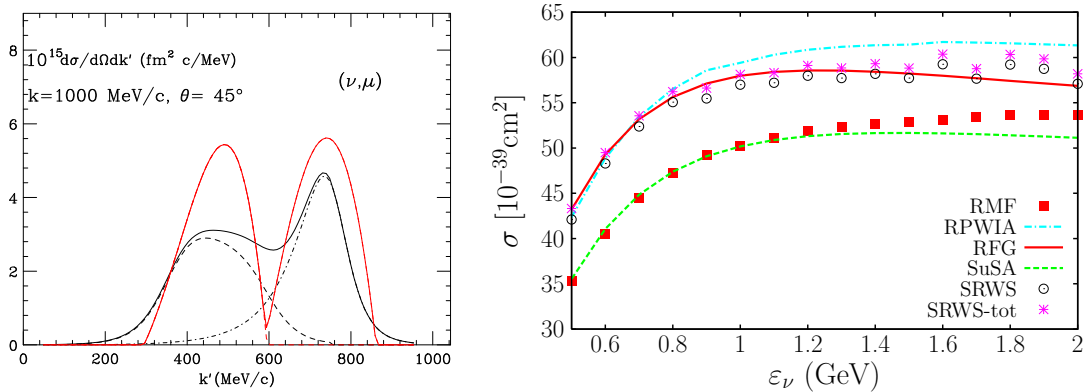


Figure 2. Left: CC neutrino reaction cross sections on ^{12}C versus the outgoing muon momentum k' , showing a comparison of the SuSA results (black online) with the RFG (red online); the separate QE and Δ contributions are shown with dashed lines. Right: integrated QE cross section versus the neutrino energy evaluated in different models.

Concerning neutral current neutrino reactions, it has been proved in Ref. [7] that, although the kinematics is not the same of (e, e') reactions because the outgoing detected particle is the knocked nucleon instead of the lepton, the SuSA approach can still be used in the QE channel to predict cross sections. The result is qualitatively similar to the CC case, namely the SuSA predictions are lower the RFG and the response extends to a wider region. As anticipated an interesting feature of NC reactions is their sensitivity to the strangeness content of the nucleon, which allows in principle to extract informations on the strange hadronic form factors by different

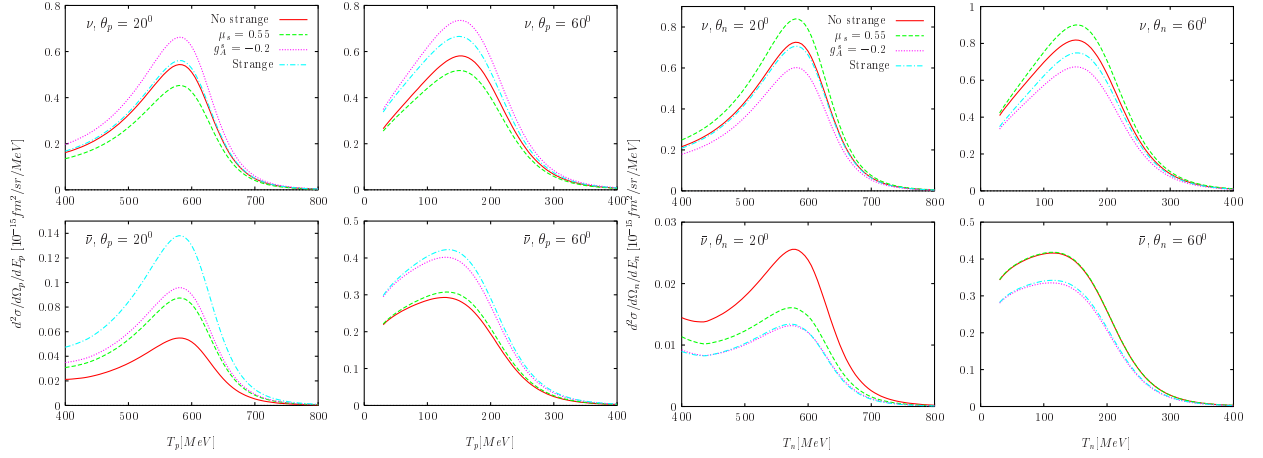


Figure 3. NC neutrino (upper panels) and antineutrino (lower panels) cross sections for proton (left) and neutron (right) knockout. The effect of strangeness is shown in the various curves.

combinations of neutrino and antineutrino scattering off protons and neutrons [13, 14, 15]. This is illustrated in the examples of Figs. 3, where it is seen that for proton knockout (left panels) the magnetic strangeness decreases (increases) the ν ($\bar{\nu}$) cross section, while the axial strangeness increases both ν and $\bar{\nu}$ cross sections. For neutron knockout (right panels) and ν scattering the situation is reversed with respect to p-knockout, while for $\bar{\nu}$ scattering the effect of magnetic strangeness is very small due to cancellation between the vector and axial-vector responses.

4. Microscopic origin of the superscaling function

In this section we will briefly illustrate the results of two relativistic models which, although sensibly different, seem to reproduce the basic properties of the experimental quasielastic superscaling function, namely a scaling behaviour of both first and second kind and a long high energy tail.

The first model is the Relativistic Mean Field model, based on a Lagrangian containing strong scalar and vector potentials (corresponding to σ , ω and ρ mesons) and describing the bound nucleon states as self-consistent Dirac-Hartree solutions. The final state interactions (FSI) are described in distorted wave impulse approximation using the same relativistic potentials [8]. As can be seen in Fig. 4 (left panel) the RMF model provides the correct amount of asymmetry, unlike other relativistic models, also shown in the same plot. These correspond to the absence of FSI (RPWIA) and to a treatment of FSI through a real optical potential (rROP). It clearly emerges from the results that not only relativity, but also a consistent treatment of the initial and final states are required in order to get the observed asymmetry of the scaling function. Moreover, as shown in Ref. [8], the model fulfills superscaling with good accuracy.

A completely different model, which we will refer to as “BCS-like”, has been shown to give very similar results [9], as illustrated in Fig. 4 (right panel). It is a simple covariant extension of RFG which accounts for NN correlations through the following wave functions

$$|\Phi\rangle = \prod_k (u_k + v_k a_{k\uparrow}^\dagger a_{-k\downarrow}^\dagger) |0\rangle \quad \text{and} \quad |D(p)\rangle = \frac{1}{|v_p|} a_{p\uparrow} \prod_k [u_k + v_k a_{k\uparrow}^\dagger a_{-k\downarrow}^\dagger] |0\rangle \quad (8)$$

for the initial and final states, respectively. The v_k -coefficients are taken phenomenologically as Fermi-Dirac distributions with one free parameter β , controlling the tail of the momentum

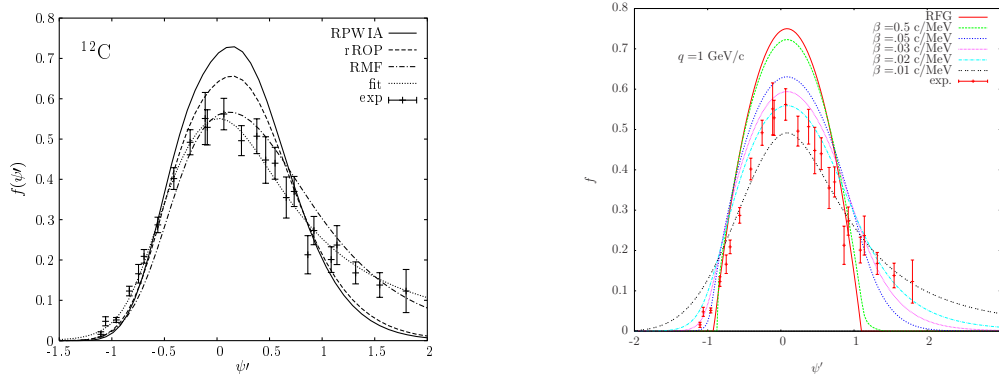


Figure 4. Left: QE superscaling function f evaluated in the RMF model compared with other models (see text); right: f in the BCS-like model for different values of the parameter β .

distribution v_k^2 . The associated superscaling function f turns out to be asymmetric in ψ , the asymmetry increasing with the value of β , and to reproduce the data for values of $\beta \simeq 0.02$ c/MeV. The superscaling properties of the BCS-like model have been explored in Ref. [9], where it was shown that both kinds of scaling are good at the QEP and broken to some degree at the right and left of it.

5. Scaling Violations

At low momentum and energy transfer (which can be defined approximately by $q < 400$ MeV/c and $\omega < 50$ MeV) the scaling approach is bound to fail because collective effects, like giant resonances, become important. However even at higher energies scaling violations are observed and it is very interesting to understand their origin.

Among other possible contributions, like *e.g.* short range correlations, meson-exchange currents (MEC) can certainly play a significant role in breaking superscaling in the transverse channel. The MEC, being two-body currents, contribute to both the 1p-1h and the 2p-2h sectors of the response and their calculation is far from trivial in a relativistic context. Moreover in order to preserve gauge invariance, in parallel with the pure MEC diagrams, where the virtual photon attaches to the exchanged meson, it is necessary to take into account the corresponding correlation diagrams, where the photon attaches to the nucleon. Up to now an exact gauge invariant relativistic calculation has been performed only in the RFG system and in the 1p-1h channel [16, 17, 18]. Here the diagrams are the ones shown in Fig. 5, where thick lines in (d)-(g) represent either a nucleon or a Δ . It turns out that the diagrams involving the Δ give the dominant contribution and they break both kinds of scaling, as illustrated in the right panel of Fig. 5. Moreover a recent calculation [19] performed in a semi-relativistic shell model essentially equivalent to the RMF with FSI has shown that the MEC contribution to the high energy tail of the response can become very large due to the dynamical nature of the pion propagator, an effect which is emphasized by the presence of FSI.

In the 2p-2h sector the pure MEC have been calculated on the RFG basis [20] and shown to give a substantial contribution at high negative and positive values of ψ , but a full gauge invariant calculation is still missing.

6. Conclusions

We have shown how the superscaling properties of (e, e') data can be exploited to predict charged and neutral current neutrino scattering cross sections and we have proposed two microscopic

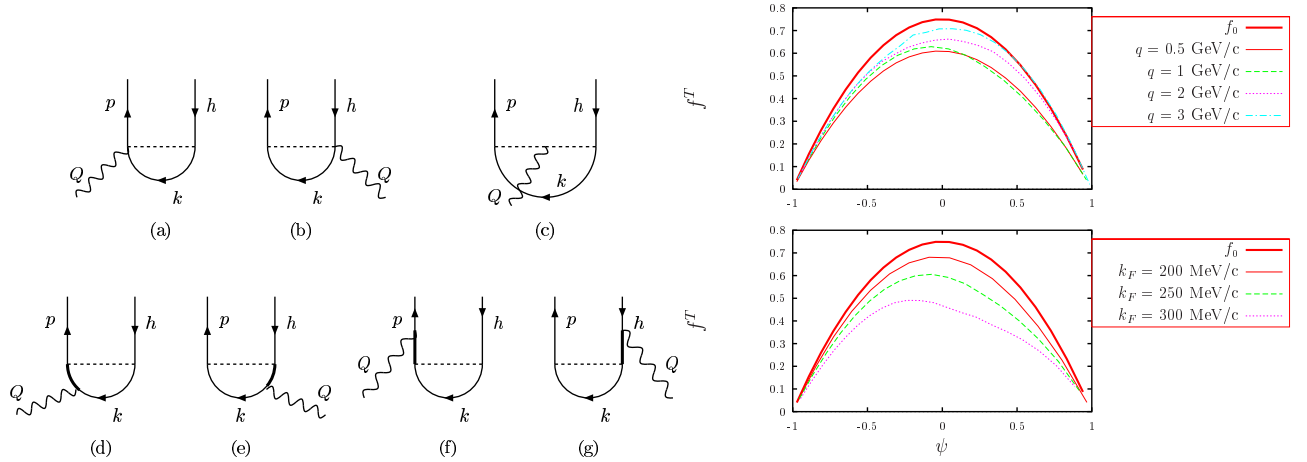


Figure 5. 1p-1h MEC diagrams and results for f in the RFG (f_0) and including the Δ -MEC diagram for different values of q (upper panel) and k_F (lower panel).

relativistic models, the RMF model and the BCS-like correlated Fermi gas, which are capable of reproducing the experimental superscaling function, in particular its long high energy tail.

However, in order to assess the applicability of the SuSA approach and eventually improve the method we need not only to justify the microscopic origin of superscaling but also to understand its violations, in particular the ones associated with meson exchange currents. This has been partially accomplished in recent work [21] and more effort will be done in this direction in order to provide a consistent description of the nuclear dynamics in the quasielastic, resonance and deep inelastic regions.

Acknowledgments

The work presented here is the result of collaborations with J.E. Amaro, J.A. Caballero, R. Cenni, T.W. Donnelly, C. Maieron, A. Molinari, I. Sick and J.M. Udias.

References

- [1] O. Benhar, D. Day and I. Sick, arXiv:nucl-ex/0603032.
- [2] G. B. West, Phys. Rept. **18** (1975) 263.
- [3] W. M. Alberico *et al.*, Phys. Rev. C **38** (1988) 1801.
- [4] D. B. Day, J. S. McCarthy, T. W. Donnelly and I. Sick, Ann. Rev. Nucl. Part. Sci. **40** (1990) 357.
- [5] T. W. Donnelly and I. Sick, Phys. Rev. Lett. **82** (1999) 3212.
- [6] J. E. Amaro *et al.*, Phys. Rev. C **71** (2005) 015501.
- [7] J. E. Amaro, M. B. Barbaro, J. A. Caballero and T. W. Donnelly, Phys. Rev. C **73** (2006) 035503.
- [8] J. A. Caballero *et al.*, Phys. Rev. Lett. **95** (2005) 252502.
- [9] M. B. Barbaro, R. Cenni, T. W. Donnelly and A. Molinari, Phys. Rev. C **78** (2008) 024602.
- [10] J. Jourdan, Nucl. Phys. A **603** (1996) 117.
- [11] J. E. Amaro, M. B. Barbaro, J. A. Caballero and T. W. Donnelly, Phys. Rev. Lett. **98** (2007) 242501.
- [12] T. Katori [MiniBooNE Collaboration], Proceedings of NUINT09, arXiv:0909.1996 [hep-ex].
- [13] M. B. Barbaro *et al.*, Phys. Rev. C **54** (1996) 1954.
- [14] W. M. Alberico *et al.*, Phys. Lett. B **438** (1998) 9.
- [15] A. Meucci, C. Giusti and F. D. Pacati, Nucl. Phys. A **773** (2006) 250.
- [16] J. E. Amaro *et al.*, Nucl. Phys. A **643** (1998) 349.
- [17] J. E. Amaro *et al.*, Phys. Rept. **368** (2002) 317.
- [18] J. E. Amaro *et al.*, Nucl. Phys. A **723** (2003) 181.
- [19] J. E. Amaro *et al.*, arXiv:0906.5598 [nucl-th].
- [20] A. De Pace *et al.*, Nucl. Phys. A **726** (2003) 303.
- [21] C. Maieron *et al.*, Phys. Rev. C **80** (2009) 035504.